

A Ketogenic & Low-Protein Diet Slows Retinal Degeneration in rd10 Mice

Renee C. Ryals¹, Samuel J. Huang¹, Dahlia Wafai¹, Claire Bernert¹, William Steele¹, Makayla Six¹, Shasank Bonthala¹, Hope Titus¹, Paul Yang¹, Melanie Gillingham², and Mark E. Pennesi¹

¹ Department of Ophthalmology, Casey Eye Institute, Oregon Health & Science University, Portland, OR, USA

² Department of Molecular and Medical Genetics, Oregon Health & Science University, Portland, OR, USA

Correspondence: Renee C. Ryals, Casey Eye Institute, Oregon Health & Science University, Portland, OR, USA. e-mail: ryals@ohsu.edu

Received: May 11, 2020

Accepted: September 23, 2020

Published: October 14, 2020

Keywords: ketogenic diet; protein deficiency; retinal degeneration; neuroprotection; rd10 mouse

Citation: Ryals RC, Huang SJ, Wafai D, Bernert C, Steele W, Six M, Bonthala S, Titus H, Yang P, Gillingham M, Pennesi ME. A ketogenic & low-protein diet slows retinal degeneration in rd10 mice. *Trans Vis Sci Tech.* 2020;9(11):18, <https://doi.org/10.1167/tvst.9.11.18>

Purpose: Treatments that delay retinal cell death regardless of genetic causation are needed for inherited retinal degeneration (IRD) patients. The ketogenic diet is a high-fat, low-carbohydrate diet, used to treat epilepsy, and has beneficial effects for neurodegenerative diseases. This study aimed to determine whether the ketogenic diet could slow retinal degeneration.

Methods: Early weaned, rd10 and wild-type (WT) mice were placed on either standard chow, a ketogenic diet, or a ketogenic & low-protein diet. From postnatal day (PD) 23 to PD50, weight and blood β -hydroxybutyrate levels were recorded. Retinal thickness, retinal function, and visual performance were measured via optical coherence tomography, electroretinography (ERG), and optokinetic tracking (OKT). At PD40, serum albumin, rhodopsin protein, and phototransduction gene expression were measured.

Results: Both ketogenic diets elicited a systemic induction of ketosis. However, rd10 mice on the ketogenic & low-protein diet had significant increases in photoreceptor thickness, ERG amplitudes, and OKT thresholds, whereas rd10 mice on the ketogenic diet showed no photoreceptor preservation. In both rd10 and WT mice, the ketogenic & low-protein diet was associated with abnormal weight gain and decreases in serum albumin levels, 27% and 56%, respectively. In WT mice, the ketogenic & low-protein diet was also associated with an ~20% to 30% reduction in ERG amplitudes.

Conclusions: The ketogenic & low-protein diet slowed retinal degeneration in a clinically relevant IRD model. In WT mice, the ketogenic & low-protein diet was associated with a decrease in phototransduction and serum albumin, which could serve as a protective mechanism in the rd10 model. Although ketosis was associated with protection, its role remains unclear.

Translational Relevance: Neuroprotective mechanisms associated with the ketogenic & low-protein diet have potential to slow retinal degeneration.

Introduction

Retinitis pigmentosa (RP) typically leads to the progressive degeneration of rod photoreceptors, followed by gradual loss of the cone photoreceptors, which results in initial symptoms of night-blindness and peripheral vision loss, followed by severe tunnel vision and ultimately profound loss of visual acuity.¹ Due to this devastating, progressive vision loss, RP has

been associated with a higher prevalence of anxiety and depression impacting the quality of life of patients.² With a prevalence of one in 4000 worldwide, this rare disorder is just one subclass of a large family of inherited retinal degenerations.^{1,3} In 2017, the Food and Drug Administration approved an AAV2-based gene augmentation therapy, voretigene neparvovec-rzyl (Luxturna), for patients harboring biallelic mutations in RPE65.^{4,5} However, because of the multitude of genes causing RP, as well as the many years and high

cost of developing gene-specific therapies, a gene-independent approach is needed. Several therapeutic strategies are being explored to fulfill this need, and neuroprotective agents are one of the most promising approaches for broad treatment.^{1,6}

Dietary supplementation with vitamin A, docosahexaenoic acid (DHA), and lutein have been thoroughly investigated for visual benefits in patients with RP.¹ Although reported visual improvements remain controversial, oral supplementation has been demonstrated to be safe, and dietary interventions continue to be an important avenue for treatment. The ketogenic diet has been used for more than 100 years to treat epilepsy.^{7–10} By eating a high-fat, low-carbohydrate diet, there is a shift from glycolysis to fatty acid oxidation that generates ketones and creates a state of ketosis.^{7,8,11} To this day, the exact anticonvulsant action of the ketogenic diet remains unclear, but several mechanisms have now been implicated to reduce neuronal excitability.⁷ More recently, animal and clinical studies have shown that the ketogenic diet has beneficial effects for neurodegenerative disorders including Parkinson's disease and Alzheimer's disease.^{8,12} Because the retina is part of the central nervous system, we sought to investigate the potential of a ketogenic diet to induce neuroprotection in photoreceptor degenerations.

There is a precedent to suggest that ketone metabolism plays an important role in retinal homeostasis.^{13–15} In the retinal pigment epithelium (RPE), degraded lipids from the shed photoreceptor outer segments are metabolized via β -oxidation to generate acetyl CoA, an important source of energy.^{14,15} Furthermore, the RPE converts acetyl CoA into the ketone, β -hydroxybutyrate (BHB), which can be shuttled back to the photoreceptors and used as an additional energy source.¹⁴ BHB also activates the G-protein coupled receptor, GPR109A, known to regulate inflammation, stress resistance, and longevity.¹⁶ This downstream signaling may play a role in increasing anti-inflammatory proteins, increasing mitochondrial biogenesis/function, reducing oxidative stress, and decreasing expression of proapoptotic factors.^{8,17–21} Taken together, BHB has been explored as a neuroprotective target. Previous work has shown that a ketogenic diet with approximately 80% fats, 8% proteins, and <1% carbohydrates protected retinal ganglion cells from N-methyl D-aspartate-induced damage.¹³

We hypothesized that inducing ketosis through ketogenic diet administration would elicit neuroprotection of photoreceptors. To test this hypothesis, we evaluated two different ketogenic diets in rd10 mice, a relevant and well-characterized genetic model of RP.²²

We found that a ketogenic diet with reduced protein content decreases phototransduction and protects the retina from degeneration.

Materials and Methods

Animals

Wild-type C57BL/6J (WT) (Cat no. 000664) and rd10 (Cat no. 004297) breeders were obtained from The Jackson Laboratory (Bar Harbor, ME, USA). C57BL/6J were chosen as a WT control to match the genetic background of the rd10 mice (B6.CXB1-*Pde6b*^{rd10/J}) purchased from The Jackson Laboratory. Pups of both sexes were either weaned at postnatal day (PD)21 (standard) or PD14/15 (early wean). Mice were housed in standard conditions under a 12/12-hour light-dark cycle. All experiments were approved by the Institutional Animal Care and Use Committee at OHSU, and adhered to the ARVO Statement for the Use of Animals in Ophthalmic and Vision Research.

Diets

Experimental rd10 and WT animals were early weaned at PD14/15 and provided either standard chow, a ketogenic diet, or a ketogenic & low-protein diet. To control for early weaning, additional rd10 and WT animals were weaned at the standard PD21 timepoint and provided standard chow. All groups are listed in [Table 1](#). [Table 2](#) lists fat, protein, and carbohydrate percentages (by weight) for each diet. Both ketogenic diets had high fat content (>65% by weight) and low carbohydrate content (<3.5%), but varied in protein content. We chose one diet that meets minimum protein requirements for mice (~15%),²³ which will be referred to as the ketogenic diet, and one diet with a low protein content (~8%), which will be referred to as a ketogenic & low-protein diet. [Table 3](#) lists fatty acid composition for the two different ketogenic diets. Standard chow, PicoLab Laboratory Rodent Diet 5L0D (LabDiet, St. Louis, MO, USA), was provided by the OHSU Department of Comparative Medicine. The ketogenic diet was purchased from ENVIGO (TD.96355; Madison, WI, USA). The ketogenic & low-protein diet was purchased from BioServ (F3666; Flemington, NJ, USA). In addition to the low protein content, the BioServ F3666 diet is reported to have low choline and methionine levels.²⁴ All diets were administered daily, so animals could eat ad libitum. Water was also available ad libitum.

Table 1. List of Experimental Groups

Animal Strain	Wean Date	Diet	Group Name
C57BL/6J	PD21	Standard Chow	WT-W21-SC
rd10	PD14/15	Ketogenic & Low-Protein	rd-W14/15-KLP
rd10	PD14/15	Ketogenic	rd-W14/15-K
rd10	PD14/15	Standard Chow	rd-W14/15-SC
rd10	PD21	Standard Chow	rd-W21-SC
C57BL/6J	PD14/15	Ketogenic & Low-Protein	WT-W14/15-KLP
C57BL/6J	PD14/15	Standard Chow	WT-W14/15-SC

Table 2. List of Diets and Their Composition

Diet	Company	Catalog no.	Fat (%)	Protein (%)	Carbohydrate (%)
Standard Chow	PicoLab	5L0D	4.5	23.0	46.5
Ketogenic	Envigo	TD.96355	67.4	15.3	0.5
Ketogenic & Low Protein	BioServ	F3666	75.1	8.6	3.2

*Macronutrient content expressed as percent by weight (proximate profile).

Table 3. Fatty Acid Composition in the Two Ketogenic Diets

Fatty Acid Class	Ketogenic Diet (g/kg)	Ketogenic & Low-Protein Diet (g/kg)
SFA	170.4	303.4
MUFA	141.1	287.6
PUFA	349.1	121.6
Caprylic (C8:0)	0.0	2.4
Capric (C10:0)	0.0	5.5
Lauric (C12:0)	0.0	6.1
Myristic (C14:0)	0.0	21.0
Palmitic (C16:0)	110.0	168.4
Palmitoleic (C16:1)	0.0	14.9
Stearic (C18:0)	60.4	86.1
Oleic (C18:1)	141.4	266.7
Linoleic (C18:2)	313.0	114.9
Linolenic (C18:3)	36.0	6.7

SFA-saturated fatty acids, MUFA-monounsaturated fatty acids, PUFA-polyunsaturated fatty acids

β -hydroxybutyrate (BHB) Measurements

At PD23, PD30, PD40, and PD50, whole blood BHB concentrations (mmol/L) were measured using the Precision Xtra ketone monitor (Abbott, Chicago, IL, USA). Blood ketone strips were used to collect blood from the saphenous vein.

segmented using a custom-designed SD-OCT segmentation program built in IGOR Pro (IGOR Pro 6.37; WaveMetrics, Inc., Lake Oswego, OR, USA). To measure photoreceptor thickness, REC+ was defined as the thickness from the base of the RPE to the interface of the inner nuclear layer and outer plexiform layer. REC+ values from both eyes were averaged for each animal.

Spectral Domain–Optical Coherence Tomography (SD-OCT)

At specified time points, mouse retinas were imaged using SD-OCT.^{22,25} Temporal, nasal, superior, and inferior quadrants were imaged. Retinal layers were

Electroretinography (ERG)

ERG was performed as described previously.²⁶ Briefly, mice were dark-adapted overnight. Under dim red light, mice were anesthetized with ketamine

(100 mg/kg) and xylazine (10 mg/kg). Bilateral platinum electrodes were placed on the corneal surface to record the light-induced retinal potentials. The reference and ground electrodes placed subcutaneously in the forehead and tail, respectively. For rd10 animals, at PD50 (~35 days on the diet), scotopic flashes at $-1.68 \log \text{ cd} \cdot \text{s/m}^2$ and $3.39 \log \text{ cd} \cdot \text{s/m}^2$ were recorded. Then, animals were light adapted with bright white light for 10 minutes and a photopic flash at $0.82 \log \text{ cd} \cdot \text{s/m}^2$ was recorded. For WT animals, at PD30 (~15 days on the diet) and PD50 (~35 days on the diet), scotopic ERG responses were recorded at increasing light intensities from -4.34 to $3.55 \log \text{ cd} \cdot \text{s/m}^2$.

Optokinetic Tracking (OKT)

OKT thresholds were used to identify spatial frequencies of gratings (cycles/degree) which define visual performance for animals (OptoMotry; CerebralMechanics, Lethbridge, Alberta, Canada).²⁷⁻³⁰ Briefly, animals were placed on the pedestal in the OptoMotry system and given five minutes to acclimate to the new environment. A simple staircase method at 100% contrast in normal lighting conditions was used for testing. Right and left eyes were tested separately and averaged together to get one spatial frequency per animal.

Histology

At PD50, enucleated eyes were placed immediately in 4% paraformaldehyde (PFA) and incubated overnight at 4°C. Eyes were processed and embedded in paraffin for sectioning (Tissue-Tek VIP 6, Tissue-Tek TEC 5; Sakura Finetek USA, Inc., Torrance, CA, USA). Sections were cut with a microtome to a thickness of 4 μm , stained with hematoxylin-eosin, and viewed on a Leica DMI3000 B microscope (Leica Microsystems GmbH, Wetzlar, Germany). Sections of whole globes were captured with a $\times 5$ objective, and retinal insets were captured with a $\times 40$ objective.

Cone Counting

At PD50, WT and rd10 eyes were harvested and placed in 4% PFA. At 24 hours after fixation, the neural retina was dissected from the sclera and washed with phosphate buffered saline solution (PBS). Neural retinas were placed in a primary antibody consisting of anti-cone arrestin (1:1000, ab15282; Millipore, Burlington, MA, USA), 0.3% Triton X-100, 5% donkey serum and PBS for one week. Tissues were rinsed and placed in a secondary antibody containing goat

anti-rabbit Alexa 647 (1:800, Cat no. A31573; Life Technologies, Eugene, OR, USA), 5% donkey serum and sodium azide. After three days, retinas were rinsed again and placed in a DAPI solution for 24 hours. Neural retinas were cut into four leaflets and mounted on a slide. For imaging of the entire flat mount, a BZ-X700 fluorescence microscope equipped with Plan Apochromat 20X objective (Keyence, Itasca, IL, USA) was used to capture tiled images, and the BZ-X Analyzer software (Keyence) was used for image stitching. Retinas were imaged with a white light laser confocal microscope (TCS SP8 X; Leica Microsystems, Buffalo Grove, IL, USA). Z-stacks (spanned 45 μm with 1 μm interval) were collected using a $\times 20$ objective capturing nasal, temporal, inferior, superior areas of the retina. Cone outer segments were counted using the automated analyze particles tool in ImageJ software (version 1.49; National Institutes of Health, Bethesda, MD, USA). Cone counts from four areas of the retina were performed by three different individuals and averaged. There were three animals in each group, and the experiment was repeated twice.

Quantitative Polymerase Chain Reaction (RT-qPCR)

Expression of phototransduction genes (Rho, Gnat1, Pde6 β , Opnsw, Gnat2, Gnb3) were assessed in the neural retina after animals were on the diet for 25 days. Primers for all analyzed genes are listed in Table 4. Neural retina from both right and left eyes were combined and total RNA was extracted using an RNeasy Mini Kit (Qiagen, Hilden, Germany) and 1 μg was converted to cDNA with iScript cDNA synthesis kit (Bio-Rad, Hercules, CA, USA). SYBR Green (Dynamo HS SYBR Green qPCR kit, F410L; ThermoFisher Scientific, Waltham, MA, USA) was used to perform qPCR on the QuantStudio 3 Real-Time PCR System (Applied Biosystems, Foster City, CA, USA). Each group contained 4 animals and the experiment was repeated twice. The housekeeping gene, eukaryotic translation elongation factor 2 (Eef2), was used as a reference gene. Ct values >35 were set as 35. Relative gene expression was analyzed using the $2^{-\Delta\text{Ct}}$ method.³¹ Fold change ≥ 2 was considered as biologically significant.

Western Blots

Retinal rhodopsin and β -actin protein content was measured via Western blot at PD40.³² Total protein

Table 4. qPCR Primer Sequences and Conditions

Gene	Primer (5' to 3')	Annealing Temp (°C)	Amplicon Size (bp)
<i>Rho</i>	<i>Fwd</i> : TGAGGATAGCACCCATGCAA <i>Rev</i> : GGCGCAGCTTCTTGAATCTC	62	397
<i>Gnat1</i>	<i>Fwd</i> : CCCACTGAGCAGGACGTGTT <i>Rev</i> : AGCGCAGCGATGAAAATGAT	62	176
<i>Pde6β</i>	<i>Fwd</i> : TCCTCTGGTCAGCCAATAAGGT <i>Rev</i> : TGTTCTGGGCTGAGTATG	62	200
<i>Opnsw</i>	<i>Fwd</i> : GAGGCCTTCTGGGCTCTGTA <i>Rev</i> : ATGAACCTGCTCCAGCCAAA	62	200
<i>Gnat2</i>	<i>Fwd</i> : CCAGCTGGACCGGATTACAG <i>Rev</i> : CAGGTGACTCCCTCGAAGCA	62	189
<i>Gnb3</i>	<i>Fwd</i> : GGGACATCTGGCCAAGATCTAT <i>Rev</i> : TCCTGCGAGGCACTTACGA	62	72
<i>Eef2</i>	<i>Fwd</i> : TGTCAGTCATCGCCCATGTG <i>Rev</i> : CATCCTTGCGAGTGTCACTGA	62	123

was extracted, and 100 μ g of protein was loaded into a 4% to 20% tris-glycine gel. After transfer, membranes were blocked for one hour, incubated overnight in primary antibodies (anti-rhodopsin Rho 4D2, ab98887 and anti-actin, ab3280; Abcam, Cambridge, UK), and incubated in a secondary antibody (1:15,000, goat anti-mouse IRDye 800CW, 925-32210; LICOR, Lincoln, NE, USA). Blots were imaged with an infrared imaging system (Odyssey, Odyssey 2.1 software; LICOR). The optical density of each band was measured with Odyssey software, rhodopsin intensity values were normalized with β -actin and fold changes were compared among groups ($n = 2-4$ in each group). This experiment was repeated twice.

Serum Albumin

A mouse albumin enzyme-linked immunosorbent assay kit (ab207620; Abcam) was used to measure serum albumin concentrations 25 days after continuous diet administration. Plasma was collected from whole blood. A 1:10 million dilution was performed on all plasma samples. Subsequently, a serial dilution of a 10,000 pg/mL albumin stock was prepared at 4000, 2000, 1000, 500, 250, 125, 62.5, and 0 pg/mL. Samples and standards were pipetted into provided antibody coated well plate strips (in duplicates or triplicates). Samples, and standards underwent a series of incubations and washes before measuring absorbance at 450 nm using a Victor X5 Multilabel Plate reader (PerkinElmer, Waltham, MA, USA). Rd10 and WT groups contained four animals each. The rd10 experiment was repeated twice and the WT experiment was repeated three times.

Statistics

For photoreceptor thickness, ERG amplitudes, and visual performance measurements right eye and left eye values were averaged to report one value per animal. For all photoreceptor thickness, blood ketone concentration, weight, and visual performance measurements, which were repeated measures from multiple cohorts, differences between groups at each time point were calculated using a two-way analysis of variance (ANOVA) mixed-effects analysis and Tukey's multiple comparisons test (Prism 8 software; GraphPad Software, La Jolla, CA, USA). For WT scotopic ERG analysis, a two-way repeated measures ANOVA and Tukey's multiple comparisons test was used to compare groups. For rd10 ERG analysis, outer segment counting, albumin concentrations, and WT western blot analysis, unpaired *t*-tests were used to compare differences between groups. For rd10 western blot analysis, an ordinary one-way ANOVA and Tukey's multiple comparisons test was used for comparisons. Some data is presented as mean \pm SEM, while some is presented as mean \pm SD. Data presentation and statistical analysis used is specified in each figure legend. A $P < 0.05$ was considered as statistically significant.

Results

A Ketogenic & Low-Protein Diet Slows Retinal Degeneration in rd10 Mice

To determine whether a ketogenic diet has neuroprotective effects for retinal degeneration, rd10 mice

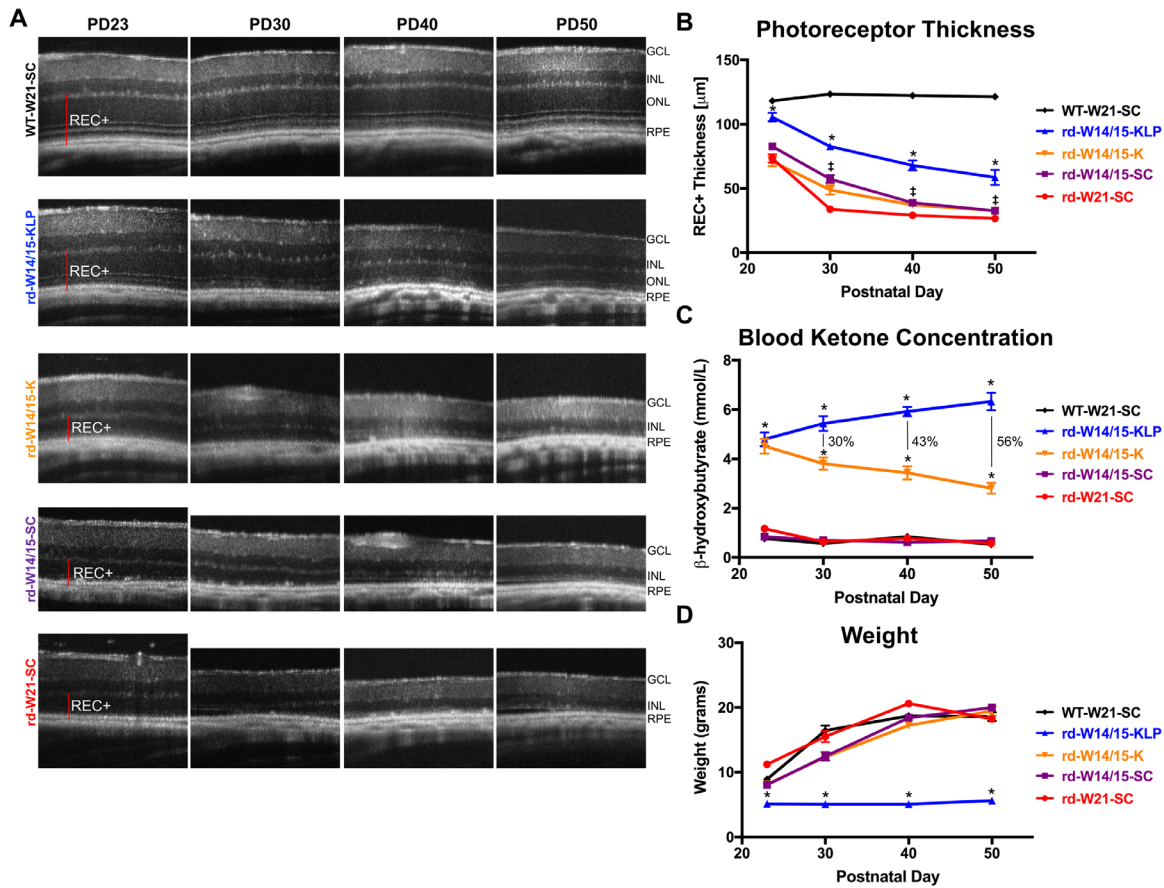


Figure 1. A ketogenic & low-protein diet slows retinal degeneration in the rd10 mouse. **(A)** Representative SD-OCT images of nasal retina from right eyes of animals. **(B)** REC+ (photoreceptor + RPE) thickness, obtained from segmentation of SD-OCT images. Data are reported as average \pm SEM. A two-way ANOVA, mixed-effects model demonstrated a main effect of treatment group, $F(4, 82) = 99.66$, $P < 0.0001$. The ketogenic & low-protein diet significantly preserved photoreceptors in rd10 retinas from P23 to P50 (Tukey's multiple comparisons test, $*P < 0.05$). Early weaning rd10 animals had a modest, but statistically significant effect as well (Tukey's multiple comparisons test, $\ddagger P < 0.05$). The sample size for each group at each time point is reported in Supplementary Table S1. **(C)** Blood BHB levels measured with the Precision Xtra ketone monitor. Data are reported as average \pm SEM. A two-way ANOVA, mixed-effects model demonstrated a main effect of treatment group ($F(4, 109) = 416.5$, $P < 0.0001$). Both ketogenic diets significantly induced ketosis in rd10 mice at all time points (Tukey's multiple comparisons test, $*P < 0.05$). The percent difference in BHB levels between the two ketogenic diets is reported. The sample size for each group at each time point is reported in Supplementary Table S1. **(D)** Animal weights are reported as average \pm SEM. A two-way ANOVA, mixed-effects model demonstrated a main effect of treatment group, $F(4, 122) = 124.2$, $P < 0.0001$. rd10 mice on the ketogenic & low-protein diet failed to follow normal weight gain patterns (Tukey's multiple comparisons test, $*P < 0.05$). The sample size for each group at each time point is reported in Supplementary Table S1. GCL, ganglion cell layer; INL, inner nuclear layer.

were weaned at PD14/15 and placed on either standard chow, the ketogenic diet, or the ketogenic & low-protein diet until PD50. Experimental groups are listed in Table 1. Over time photoreceptor thickness, blood β -hydroxybutyrate (BHB) levels, and animal weights were monitored (Fig. 1). Retinal images showed that rd10 animals (rd-W21-SC) underwent photoreceptor degeneration by PD23, which continued out to PD50. By PD50, the outer nuclear layer (ONL), as well as photoreceptor inner and outer segments were completely diminished (Fig. 1A). When rd10 mice were early weaned and placed on standard chow (rd-W14/15-SC), photoreceptor thickness was

significantly preserved at PD30 (1.6-fold), PD40 (1.2-fold), and PD50 (1.1-fold) compared to rd10 mice weaned at PD21 (rd-W21-SC) (Figs. 1A, 1B; $\ddagger P < 0.05$). When early weaned rd10 mice were then placed on the ketogenic & low-protein diet (rd-W14/15-KLP), photoreceptor preservation was significantly more robust, increasing by 1.2-fold at PD23, 1.5-fold at PD30, 1.9-fold at PD40, and 1.9-fold at PD50 (Figs. 1A, 1B; $*P < 0.05$). In contrast, when early weaned rd10 mice were placed on the ketogenic diet (rd-W14/15-K), there were no changes in photoreceptor thickness compared to early weaned rd10 animals on standard chow (rd-W14/15-SC) (Figs. 1A, 1B;

$P > 0.05$). We investigated the potential for a sex-specific protective effect of the ketogenic & low-protein diet using three-factor ANOVA. As expected, there were significant main effects for age ($F(3,101) = 66.242$, $P < 2e-16$) and diet ($F(1,101) = 107.419$, $P < 2e-16$) on photoreceptor thickness. However, there was no main effect of sex ($P = 0.545$) and no significant interactions between independent variables (Supplementary Fig. S1). To measure the induction of ketosis, BHB, the main ketone product of ketogenesis and the main substrate for ketone metabolism, was measured (Fig. 1C). At all-time points, both ketogenic diets significantly increased blood BHB concentrations (Fig. 1C, $*P < 0.05$). Interestingly, BHB levels were significantly higher by 30% (PD30), 43% (PD40), and 56% (PD50) in ketogenic & low-protein animals compared to ketogenic animals (Fig. 1C). Animals on the ketogenic & low-protein diet failed to gain weight compared to all other groups (Fig. 1D, $*P < 0.05$).

As the only diet to show preservation of photoreceptors, we decided to further characterize the protection gained by the ketogenic & low-protein diet (Fig. 2). First, OKT thresholds were measured in normal lighting conditions at PD30 and PD50. At PD30, there was an appreciable, but not significant increase in spatial frequency for rd10 animals that were early weaned (rd-W14/15-SC). However, by PD50 that increase diminished, and only animals on the ketogenic & low-protein diet (rd-W14/15-KLP) had significant preservation of visual performance (Fig. 2A, $*P < 0.05$). In addition, at PD50, scotopic and photopic ERGs were recorded. As expected with the *Pde6 β* mutation,³³ rod-mediated ERG responses were not preserved in the rd10 mouse (Supplementary Fig. S2A, $P > 0.05$). However, cone-mediated b-wave amplitudes recorded from the photopic flash and the maximum scotopic flash were 1.8-fold higher as a result of the ketogenic & low-protein diet (Fig. 2B and Supplementary Fig. S2B, $*P < 0.05$). Consistent with this, when cone outer segments were counted from rd-W14/15-KLP whole mount retina, there was a 1.6-fold increase in the number of cone outer segments compared to rd-W14/15-SC (Fig. 2C, $*P < 0.05$, Supplementary Fig. S3, Supplementary Movies S1–S3). Histology of eyes harvested from early weaned rd10 mice on the ketogenic & low-protein diet demonstrate structural maintenance of photoreceptor cell bodies, inner segments and outer segments throughout the entire retina compared to animals on standard chow (Fig. 2D).

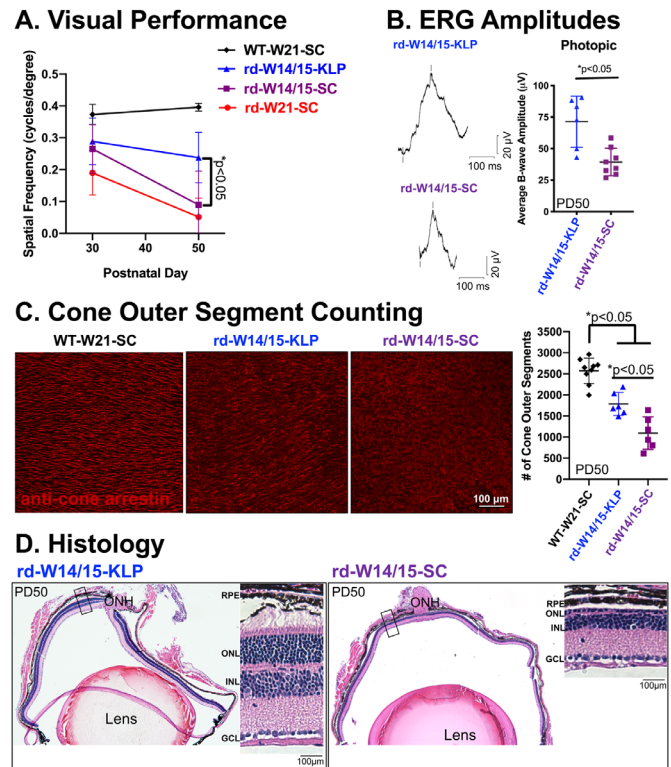


Figure 2. Cone preservation is evident in rd10 mice on the ketogenic & low protein diet. **(A)** Optokinetic tracking thresholds were measured in normal lighting conditions to evaluate visual performance. Data are reported as average \pm SD. A two-way ANOVA, mixed-effects model demonstrated a main effect of treatment group ($F(3, 24) = 17.3$, $P < 0.0001$). At PD50, spatial frequencies were increased by 2.6-fold in rd10 mice due to the ketogenic & low protein diet (Tukey's multiple comparisons test, $*P < 0.05$). WT-W21-SC $n = 4$, rd-W14/15-KLP $n = 7-8$, rd-W14/15-SC $n = 8$, rd-W21-SC $n = 4$. **(B)** Representative ERG traces and average b-wave amplitudes from a photopic flash at $0.82 \log \text{cd} \cdot \text{s/m}^2$ show that cone function was significantly increased by 1.8-fold in rd10 mice on the ketogenic & low-protein diet. Data are reported as average \pm SD. Significance was determined with an unpaired t -test ($P = 0.0025$). rd-W14/15-KLP $n = 6$, rd-W14/15-SC $n = 8$). **(C)** Cone outer segments were counted from whole mount retina leaflets that were stained with an antibody specific for cone arrestin using a semiautomatic program in ImageJ. Data are reported as average \pm SD. An ordinary one-way ANOVA demonstrated a main effect of treatment group ($F(2,18) = 39.55$, $P < 0.001$). Rd10 mice on the ketogenic & low-protein diet had 1.6-fold more cone outer segments than rd10 mice on standard chow (Tukey's multiple comparison test, $*P < 0.05$). WT-W21-SC $n = 9$, rd-W14/15-KLP $n = 6$, rd-W14/15-SC $n = 6$. **(D)** hematoxylin-eosin images of right eyes obtained from a rd10 mouse with substantial protection on the ketogenic & low protein diet and a rd10 mouse on standard chow, highlight that photoreceptor preservation is evident throughout the entire retina. ONH, optic nerve head; GCL, ganglion cell layer; INL, inner nuclear layer.

A Ketogenic & Low-Protein Diet Reduces ERG Amplitudes in WT Mice

To investigate the mechanism of protection, we early weaned wild-type, C57BL/6J (WT) mice at PD14/15 and administered either standard chow (WT-W14/15-SC) or the ketogenic & low-protein diet (WT-W14/15-KLP) until PD50. BHB and weights were measured to ensure the diet was affecting WT (WT-W14/15-KLP) and rd10 (rd-W14/15-KLP) animals in a similar manner (Figs. 3A, 3B). Based on BHB levels, the ketogenic & low-protein diet induced ketosis to the same level in WT and rd10 animals (Fig. 3A, $P > 0.05$). Similar to rd10 mice, WT animals failed to gain weight on the ketogenic & low-protein diet. However, WT-W14/15-KLP animals were ~2 grams heavier than rd-W14/15-KLP at the PD40 and PD50 time point (Fig. 3B, PD40 $*P < 0.05$; PD50 $P > 0.05$). When comparing photoreceptor thickness between WT-W14/15-SC and WT-W14/15-KLP animals, there were no significant differences from PD23 to PD40 (Figs. 3C, 3D; $P > 0.05$). However, early weaned animals (WT-W14/15-SC) had significantly increased photoreceptor thicknesses (~6 μ m REC+) compared to WT-W21-SC animals at PD23 (Fig. 3D, $*P < 0.05$). Similar to OCT, when comparing OKT thresholds between the WT-W14/15-SC group and the WT-W14/15-KLP group, there were no significant differences from PD30 to PD40 (Fig. 3E, $P > 0.05$). Interestingly, scotopic ERG recordings showed significant decreases in a-wave and b-wave amplitudes at multiple flash intensities in WT animals on the ketogenic & low-protein diet at PD30 and PD50 (Fig. 3F, $*p < 0.05$). At the maximum light intensity, both a-wave and b-wave amplitudes were decreased by ~20% at PD30 and by ~30% at PD50, showing a progressive decline in retinal function (Fig. 3F, $*P < 0.05$).

A Ketogenic & Low-Protein Diet Reduces Serum Albumin in Both rd10 and WT Mice

Taking together the lack of weight gain and decreased ERG responses, we measured serum albumin levels, a global biomarker for protein deficiency. After 25 days of continuous ketogenic & low-protein diet administration, albumin levels were significantly reduced by 27% and 56% in rd10 and WT animals, respectively (Fig. 4A, $*P < 0.05$). Western blots captured a significant reduction in rhodopsin protein from the degenerating rd10 mouse retina (rd-W14/15-SC), which was substantially increased with the protection elicited by the ketogenic & low-protein diet (rd-W14/15-KLP) (Fig. 4B,

$*P < 0.05$). When comparing the WT-W14/15-SC and WT-W14/15-KLP groups, no changes in rhodopsin protein were observed (Fig. 4B, $P > 0.05$). Similarly, rod and cone phototransduction gene expression remained unchanged (Fig. 4C, $P > 0.05$).

Discussion

There is a critical need to develop neuroprotective strategies that slow retinal degeneration in patients with RP. These advanced strategies will allow for maintenance of vision and increase the therapeutic window for gene-specific treatments. Many gene-independent strategies have been investigated, and diet manipulation is one avenue that is currently being explored.^{1,3,34} Our study is the first to show that a ketogenic & low-protein diet slows retinal degeneration in the rd10 mouse model. Not only was the structural preservation of rods and functional restoration of cones remarkable, but these gains persisted three weeks beyond normal photoreceptor loss. We speculate that reductions in rod phototransduction and serum albumin play a role in the observed neuroprotection.

In a normal retina, light stimulates rhodopsin, and activates transducin and phosphodiesterase (PDE), leading to subsequent conversion of cGMP to GMP, which closes the Na⁺/Ca⁺² channels, and hyperpolarizes the photoreceptors.³⁵ In rods, the PDE contains α , β , and γ subunits that are responsible for converting cGMP to GMP.³⁵ The rd10 mouse harbors an autosomal missense R560C mutation in the *Pde6 β* gene, which significantly reduces and mislocalizes the PDE6 β protein in rods.³³ Overall, cGMP fails to be converted to GMP, keeping the Na⁺/Ca⁺² channels open. As influxes of Ca⁺² depolarize the mitochondrial membrane and reactive oxygen species accumulate, the mitochondrial potential collapses and cell death becomes inevitable.^{33,36} As a consequence of this, rd10 mice undergo peak photoreceptor degeneration at PD21, which continues into a complete loss of rods and a significant reduction in cones by PD60.^{22,33} To ensure ketosis was initiated before peak degeneration, which can take up to four days after diet administration, animals were early weaned and fed the ketogenic diets at PD14/15.³⁷ Interestingly, early weaning alone slowed the rate of retinal degeneration in the rd10 mouse model (Figs. 1A, 1B). Impacts were most prominent at PD30, and modest, although significant out to PD50 (Fig. 1B). To our knowledge, this is the first report demonstrating photoreceptor preservation after early weaning in the rd10 mouse. This result suggests that early weaned rd10 controls are essential. If not used,

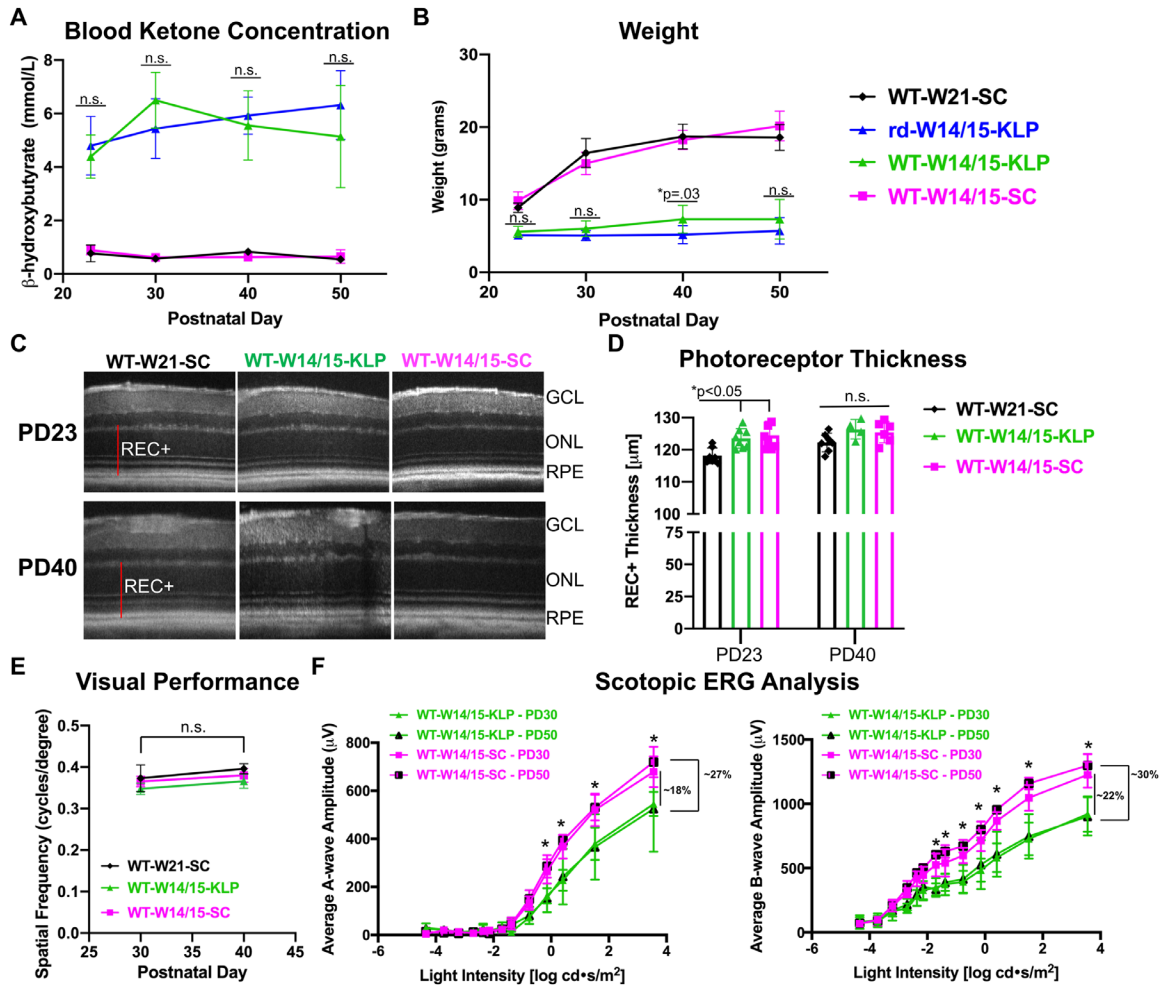


Figure 3. The ketogenic & low-protein diet reduces ERG responses in WT mice. **(A)** Blood BHB levels, measured with the Precision Xtra ketone monitor. Data are reported as average \pm SD. A two-way ANOVA, mixed-effects model demonstrated a main effect of treatment group ($F(3, 51) = 264.5, P < 0.0001$). Most importantly, these data show that the ketogenic & low-protein diet significantly induced ketosis to a similar extent in both WT and rd10 mice because there were no significant differences between WT-W14/15-KLP and rd-W14/15-KLP (Tukey's multiple comparisons test, $P > 0.05$). The sample size for each group at each time point is reported in Supplementary Table S2. **(B)** Animal weights are reported as average \pm SD over time. A two-way ANOVA, mixed-effects model demonstrated a main effect of treatment group ($F(3,67) = 381.1, P < 0.0001$). The statistics presented highlight that both WT and rd10 mice failed to follow normal gain weight patterns while on the ketogenic & low protein diet (Tukey's multiple comparisons test, n.s. $P > 0.05$, $*P < 0.05$). The sample size for each group at each time point is reported in Supplementary Table S2. **(C)** Representative SD-OCT images of nasal retina from right eyes of animals in each group. **(D)** REC+ (photoreceptor + RPE) thickness, obtained from segmentation of SD-OCT images. Data are reported as average \pm SD. An ordinary one-way ANOVA demonstrated a main effect of treatment group ($F(5, 34) = 5.08, P = 0.0014$). Most importantly, these data show that photoreceptor thickness does not change in WT animals on a ketogenic & low protein diet. However, early weaning significantly increases photoreceptor thickness at PD23 (Bonferroni's multiple comparison test, $*P < 0.05$). The sample size for each group at each time point is reported in Supplementary Table S2. **(E)** Optokinetic tracking thresholds verified that visual performance was not impacted by the ketogenic & low protein diet in WT mice. All data are reported as average \pm SD. A two-way ANOVA, mixed-effects model failed to demonstrate a main effect when analyzing the treatment group over time ($F(2, 16) = 0.19, P = 0.83$). The sample size for each group at each time point is reported in Supplementary Table S2. **(F)** Average a-wave and b-wave amplitudes at increasing light intensity are reported as mean \pm SD. A two-way repeated measures ANOVA, demonstrated a main effect of treatment group ($F(3, 17) = 7.17, P = 0.0026$ (a-wave analysis); $F(3, 17) = 18.07, P < 0.0001$ (b-wave analysis)). ERG responses are significantly decreased by $\sim 20\%$ and $\sim 30\%$ at PD30 and PD50, respectively, because of the ketogenic & low protein diet (Tukey's multiple comparison test, $*P < 0.05$). The sample size for each group at each time point is reported in Supplementary Table S2. GCL, ganglion cell layer.

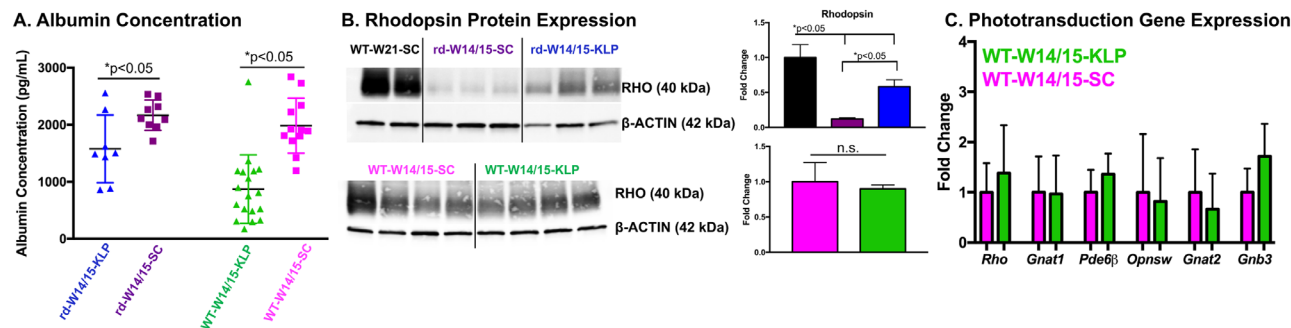


Figure 4. The ketogenic & low protein diet reduces serum albumin levels. All samples were collected at PD40 after ~25 consecutive days of diet administration. **(A)** Serum albumin levels, measured through an enzyme-linked immunosorbent assay, were significantly reduced by 27% and 56% in rd10 and C57 animals on the ketogenic & low protein diet, respectively. Data are reported as average \pm SD. Significance was determined with an unpaired *t*-test. $*P < 0.05$. rd-W14/15-KLP *n* = 8, rd-W14/15-SC *n* = 9, WT-W14/15-KLP *n* = 18, WT-W14/15-SC *n* = 12. **(B)** Western blots and the corresponding fold changes in rhodopsin demonstrate a reduction of rhodopsin protein in the degenerating rd10 mouse retina, which is significantly increased with the protection gained by the ketogenic & low protein diet. Ordinary one-way ANOVA demonstrated a main effect of treatment group ($F(2,5) = 43.66$, $P = 0.0007$, post-hoc Tukey's multiple comparisons test, $*P < 0.05$). In WT animals, no changes in rhodopsin protein were observed. Statistics were determined with an or an unpaired *t* test. Data are reported as average \pm SD. WT-W21-SC *n* = 2, rd-W14/15-SC *n* = 3, rd-W14/15-KLP *n* = 3, WT-W14/15-SC *n* = 4, WT-W14/15-KLP *n* = 4. **(C)** RT-qPCR analysis shows that rod and cone phototransduction gene expression remains unchanged. Fold change is reported as average \pm SD. WT-W14/15-SC *n* = 8, WT-W14/15-KLP *n* = 8. Fold change ≥ 2 was considered as biologically significant.

protective gains will be overreported. When postulating the mechanism of protection, we found that maternal deprivation by early weaning leads to increased corticosterone, which when administered through maternal drinking water increases retinal phosphorylation of ERK1/2 and CREB.^{38,39} Our work, as well as others, has shown that increases in corticosterone and activation of the MAPK pathway, as well as CREB, can elicit neuroprotective pathways and protect from light-induced retinopathy.^{32,40–42} In addition to activating a stress response, early weaning can delay the triggering of satiety and modulate the circadian rhythm of food intake, which was demonstrated in male Wistar rat pups out to PD100.⁴³ It is feasible that changes in behavioral satiety and food consumption can impact the retina, because recent studies have linked the gut microbiota with retinal disease.⁴⁴ Furthermore, the glucagon-like peptide-1 (GLP-1), which is an incretin hormone secreted by the gastrointestinal tract in response to food, has shown neuroprotective effects for retinal ganglion cells.⁴⁵ Extending the duration of feeding in early weaned animals could lead to increases in GLP-1.

To determine the neuroprotective mechanism of the ketogenic & low-protein diet, we evaluated its effects in WT animals. Despite normal photoreceptor thickness and visual performance, we observed ~20% to 30% decrease in scotopic a-wave and b-wave amplitudes when measured at 15 and 35 days after continuous diet administration (Fig. 3F). With an understanding of the rd10 disease mechanism, we

hypothesized that this reduction in rod-mediated phototransduction could reduce influxes of Ca^{+2} that disrupt the mitochondrial membrane, slowing the cell death process and preserving rods in the rd10 mouse model. Without restoring properly localized PDE6 β protein, rod function is unlikely to be restored in the rd10 model. However, with an increased number of rods, the rod-derived cone viability factor can help to maintain the function and viability of cone photoreceptors,⁴⁶ which is consistent with our data showing structural preservation of rods and functional preservation cones at PD50 (Fig. 2). Suppressing rod phototransduction has been investigated as a treatment for retinal degenerative diseases. Specific to the rd10 mouse model, one group disrupted the neural retina-specific leucine zipper (Nrl) gene, an important rod fate transcription factor, in postmitotic photoreceptors.⁴⁷ Rods with disrupted Nrl, exhibited reduced amounts of rod-specific gene expression and increased amounts of cone-specific gene expression, which resulted in significant preservation of the ONL and cone function.⁴⁷ Additionally, reduced rates of rhodopsin regeneration and/or reduced rhodopsin protein led to protection against light-induced retinopathy.^{40,48} Subsequently, a drug isotretinoin, which slows the synthesis of 11-cis-retinaldehyde and regeneration of rhodopsin by inhibiting 11-cis-retinol dehydrogenase, inhibited lipofuscin accumulation in a mouse model of Stargardt macular degeneration.⁴⁹ Taken together, we hypothesize that the observed reduction of rod phototransduction due to the ketogenic & low-protein diet

serves as a protective mechanism in the rd10 mouse model.

The minimum protein concentration that supports adequate growth, reproduction and lactation in the mouse is 13.6%.²³ When rodents are fed protein deficient diets, this leads to decreased body weight and reduced plasma albumin concentrations.⁵⁰ Thus the ketogenic & low-protein diet, only having 8.6% protein concentration by weight, failed to support normal weight gain after weaning (Fig. 1D) and resulted in significant reductions in serum albumin (Fig. 4A). At first, we hypothesized that this protein deficiency decreased ERG responses by reducing rhodopsin, the most abundantly expressed phototransduction protein.⁵¹ However, we did not observe changes in rhodopsin protein or gene expression between WT mice that were on the standard chow (WT-W14/15-SC) or the ketogenic & low-protein diet (WT-W14/15-KLP) (Fig. 4B). In addition, gene expression of key rod and cone phototransduction proteins were not different between the WT-W14/15-SC and WT-W14/15-KLP groups (Fig. 4C). Interestingly, it has been documented that protein deficiency and vitamin A deficiency decrease ERG amplitudes to a similar magnitude.⁵² Because albumin is an important transporter for vitamin A, diminished ERG responses may correlate to a reduced bioavailability of vitamin A.⁵² In summary, it remains unclear how protein deficiency impacted ERG responses. Additional experiments investigating the visual cycle and the functional bioefficacy of vitamin A may further our understanding.⁵³

BHB has the potential to positively impact the retina by (1) being a substrate for ketogenesis, which offers the photoreceptors an additional energy metabolism pathway,¹⁴ (2) activating GPR109A, which we and others have shown to play a role in photoreceptor protection against light-induced retinopathy,^{16,17,25} and (3) by enhancing mitochondrial biogenesis and respiration under stressed conditions.^{18,54} In this study, we show that a ketogenic diet with 67.4% fat, 0.5% carbohydrate, and 15.3% protein significantly increases systemic BHB levels in rd10 mice by 5.4-fold from PD23 to PD40 and by 4.2-fold at PD50 (Fig. 1C). These significant systemic increases in BHB did not lead to photoreceptor protection. However, we cannot definitively conclude that BHB is not playing a role in the observed neuroprotection, because animals on the ketogenic & low-protein diet had significantly increased levels in BHB by ~30% to 56% from PD30 to PD50 (Fig. 1C). It is possible that this significant increase in BHB overcomes a systemic threshold that is required for retinal neuroprotection. It is interesting to speculate whether BHB levels contribute to an additive

neuroprotective pathway, or if ketosis, which is associated with decreased energy expenditure, can decrease phototransduction.⁵⁵

The diets used in this study came from three different companies and were not ingredient-matched controls, which is one of the main limitations of the study. Ingredient differences generate confounding factors, because any ingredient changed would need to be assessed individually. Future experiments will aim to separate the confounding factors by using ingredient-matched diets from the same company and to determine the retinal impacts of global protein deficiency and ketosis, separately. Limitations of the ketogenic & low-protein diet include its potential to decrease retinal function in healthy individuals, as we saw reduced ERG responses in WT animals (Fig. 3F). However, visual performance remained stable over time (Fig. 3E), so we hypothesize that this diet may be able to slow phototransduction to an extent that is helpful in a degenerating retina without impacting overall visual performance. Other complications of the ketogenic & low-protein diet come from the resulting protein deficiency. It is unclear whether modified regimens could make this diet useful for individuals at different ages. Ultimately, hope remains that we can elucidate the neuroprotective target from this diet and localize treatments to the eye. Advances such as these would generate a paradigm shift in RP patient care.

Acknowledgments

Tissue processing and sectioning was supported by the Casey Eye Institute, Leonard Christenson Eye Pathology Laboratory.

Supported by unrestricted departmental funding from Research to Prevent Blindness (New York, NY, USA); Grant P30 EY010572 from the National Institutes of Health (Bethesda, MD, USA); K08 Career Development Award (K08 EY021186, MEP); Alcon Young Investigator Award, Foundation Fighting Blindness; Enhanced Research and Clinical Training Award (CD-NMT-0914-0659-OHSU, MEP); Career Development Award from Research to Prevent Blindness (MEP); Medical Research Foundation of Oregon (RCR), and SRA-19-088 (RCR).

Disclosure: **R.C. Ryals**, None; **S.J. Huang**, None; **D. Wafai**, None; **C. Bernert**, None; **W. Steele**, None; **M. Six**, None; **S. Bonthala**, None; **H. Titus**, None; **P. Yang**, None; **M. Gillingham**, None; **M.E. Pennesi**, None

References

1. Wang AL, Knight DK, Vu TT, Mehta MC. Retinitis Pigmentosa: Review of Current Treatment. *Int Ophthalmol Clin*. 2019;59(1):263–280.
2. Chaumet-Riffaud AE, Chaumet-Riffaud P, Cariou A, et al. Impact of retinitis pigmentosa on quality of life, mental health, and employment among young adults. *Am J Ophthalmol*. 2017;177:169–174.
3. Fahim AT, Daiger SP, Weleber RG. Nonsyndromic retinitis pigmentosa overview. In: Adam MP, Ardinger HH, Pagon RA, et al., editors. *GeneReviews [Internet]*. Seattle (WA): University of Washington, Seattle; 1993 [cited 2019 Aug 12], Available from: <http://www.ncbi.nlm.nih.gov/books/NBK1417/>.
4. Ameri H. Prospect of retinal gene therapy following commercialization of voretigene neparvovec-rzyl for retinal dystrophy mediated by RPE65 mutation. *J Curr Ophthalmol*. 2018;30(1):1–2.
5. Patel U, Boucher M, de Léséleuc L, Visintini S. Voretigene Neparvovec: An Emerging Gene Therapy for the Treatment of Inherited Blindness. In: *CADTH Issues in Emerging Health Technologies [Internet]*. Ottawa (ON): Canadian Agency for Drugs and Technologies in Health; 2016 [cited 2019 Aug 12], Available from: <http://www.ncbi.nlm.nih.gov/books/NBK538375/>.
6. Pardue MT, Allen RS. Neuroprotective strategies for retinal disease. *Prog Retin Eye Res*. 2018;65:50–76.
7. Boison D. New insights into the mechanisms of the ketogenic diet. *Curr Opin Neurol*. 2017;30(2):187–192.
8. Freeman J, Veggiotti P, Lanzi G, Tagliabue A, Perucca E, Institute of Neurology IRCCS C. Mondino Foundation. The ketogenic diet: from molecular mechanisms to clinical effects. *Epilepsy Res*. 2006;68(2):145–180.
9. Uhlemann ER, Neims AH. Anticonvulsant properties of the ketogenic diet in mice. *J Pharmacol Exp Ther*. 1972;180(2):231–238.
10. Lima PA de, Sampaio LP, de B, Damasceno NRT. Neurobiochemical mechanisms of a ketogenic diet in refractory epilepsy. *Clinics (Sao Paulo)*. 2014;69(10):699–705.
11. Maalouf M, Rho JM, Mattson MP. The neuroprotective properties of calorie restriction, the ketogenic diet, and ketone bodies. *Brain Res Rev*. 2009;59(2):293–315.
12. Włodarek D. Role of ketogenic diets in neurodegenerative diseases (Alzheimer's disease and Parkinson's disease). *Nutrients*. 2019;11(1):169.
13. Zarnowski T, Choragiewicz TJ, Schuettauf F, et al. Ketogenic diet attenuates NMDA-induced damage to rat's retinal ganglion cells in an age-dependent manner. *Ophthalmic Res*. 2015;53(3):162–167.
14. Adjianto J, Du J, Moffat C, Seifert EL, Hurley JB, Philp NJ. The retinal pigment epithelium utilizes fatty acids for ketogenesis. *J Biol Chem*. 2014;289(30):20570–20582.
15. Reyes-Reveles J, Dhingra A, Alexander D, Bragin A, Philp NJ, Boesze-Battaglia K. Phagocytosis-dependent ketogenesis in retinal pigment epithelium. *J Biol Chem*. 2017;292(19):8038–8047.
16. Rojas-Morales P, Tapia E, Pedraza-Chaverri J. β -Hydroxybutyrate: a signaling metabolite in starvation response? *Cell Signal*. 2016;28(8):917–923.
17. Rahman M, Muhammad S, Khan MA, Chen H, Ridder DA, Müller-Fielitz H, et al. The β -hydroxybutyrate receptor HCA2 activates a neuroprotective subset of macrophages. *Nat Commun*. 2014;5:3944.
18. Sullivan PG, Ripsey NA, Dorenbos K, Concepcion RC, Agarwal AK, Rho JM. The ketogenic diet increases mitochondrial uncoupling protein levels and activity. *Ann Neurol*. 2004;55(4):576–80.
19. Kennedy AR, Pissios P, Otu H, et al. A high-fat, ketogenic diet induces a unique metabolic state in mice. *Am J Physiol Endocrinol Metab*. 2007;292(6):E1724–E1739.
20. Roberts MN, Wallace MA, Tomilov AA, et al. A ketogenic diet extends longevity and healthspan in adult mice. *Cell Metab*. 2017;26(3):539–546.e5.
21. Dupuis N, Curatolo N, Benoist J-F, Auvin S. Ketogenic diet exhibits anti-inflammatory properties. *Epilepsia*. 2015;56(7):e95–e98.
22. Pennesi ME, Michaels KV, Magee SS, et al. Long-term characterization of retinal degeneration in rd1 and rd10 mice using spectral domain optical coherence tomography. *Invest Ophthalmol Vis Sci*. 2012;53(8):4644–4656.
23. Goettsch M. Comparative protein requirement of the rat and mouse for growth, reproduction and lactation using casein diets. *J Nutr*. 1960;70(3):307–312.
24. Schugar RC, Huang X, Moll AR, Brunt EM, Crawford PA. Role of choline deficiency in the fatty liver phenotype of mice fed a low protein, very low carbohydrate ketogenic diet. *PLoS ONE*. 2013;8(8):e74806.
25. Jiang D, Ryals RC, Huang SJ, et al. Monomethyl fumarate protects the retina from

- light-induced retinopathy. *Invest Ophthalmol Vis Sci.* 2019;60(4):1275–1285.
26. Suppression of cGMP-dependent photoreceptor cytotoxicity with mycophenolate is neuroprotective in murine models of retinitis pigmentosa | IOVS | ARVO Journals [Internet]. [cited 2020 Sep 7], Available from: <https://iovs.arvojournals.org/article.aspx?articleid=2770635>.
 27. McGill TJ, Douglas RM, Lund RD, Prusky GT. Quantification of spatial vision in the Royal College of Surgeons rat. *Invest Ophthalmol Vis Sci.* 2004;45(3):932–936.
 28. McGill TJ, Prusky GT, Douglas RM, et al. Discordant anatomical, electrophysiological, and visual behavioral profiles of retinal degeneration in rat models of retinal degenerative disease. *Invest Ophthalmol Vis Sci.* 2012 Sep 14;53(10):6232–6244.
 29. Wang SK, Xue Y, Rana P, Hong CM, Cepko CL. Soluble CX3CL1 gene therapy improves cone survival and function in mouse models of retinitis pigmentosa. *PNAS.* 2019;116(20):10140–10149.
 30. Xiong W, MacColl Garfinkel AE, Li Y, Benowitz LI, Cepko CL. NRF2 promotes neuronal survival in neurodegeneration and acute nerve damage. *J Clin Invest.* 2015;125(4):1433–1445.
 31. Schmittgen TD, Livak KJ. Analyzing real-time PCR data by the comparative C(T) method. *Nat Protoc.* 2008;3(6):1101–1108.
 32. Ku CA, Ryals RC, Jiang D, et al. The role of ERK1/2 activation in sarpogrelate-mediated neuroprotection. *Invest Ophthalmol Vis Sci.* 2018;59(1):462–471.
 33. Wang T, Reingruber J, Woodruff ML, et al. The PDE6 mutation in the rd10 retinal degeneration mouse model causes protein mislocalization and instability and promotes cell death through increased ion influx. *J Biol Chem.* 2018;293(40):15332–15346.
 34. Sofi F, Sodi A, Franco F, et al. Dietary profile of patients with Stargardt's disease and retinitis pigmentosa: is there a role for a nutritional approach? *BMC Ophthalmol.* 2016;16:13.
 35. Mannu GS. Retinal phototransduction. *Neurosciences (Riyadh).* 2014;19(4):275–280.
 36. Duchon MR. Mitochondria and calcium: from cell signalling to cell death. *J Physiol.* 2000;529(Pt 1):57–68.
 37. Masood W, Annamaraju P, Uppaluri KR. *Ketogenic Diet.* In: *StatPearls [Internet]*. Treasure Island (FL): StatPearls Publishing; 2020 [cited 2020 Apr 23], Available from: <http://www.ncbi.nlm.nih.gov/books/NBK499830/>.
 38. Kikusui T, Ichikawa S, Mori Y. Maternal deprivation by early weaning increases corticosterone and decreases hippocampal BDNF and neurogenesis in mice. *Psychoneuroendocrinology.* 2009;34(5):762–772.
 39. Matteucci A, Ceci C, Mallozzi C, Macri S, Malchiodi-Albedi F, Laviola G. Effects of neonatal corticosterone and environmental enrichment on retinal ERK1/2 and CREB phosphorylation in adult mice. *Exp Eye Res.* 2014;128:109–113.
 40. Wenzel A, Grimm C, Samardzija M, Remé CE. Molecular mechanisms of light-induced photoreceptor apoptosis and neuroprotection for retinal degeneration. *Prog Retin Eye Res.* 2005;24(2):275–306.
 41. Mees LM, Coulter MM, Chrenek MA, et al. Low-intensity exercise in mice is sufficient to protect retinal function during light-induced retinal degeneration. *Invest Ophthalmol Vis Sci.* 2019;60(5):1328–1335.
 42. Forkwa TK, Neumann ID, Tamm ER, Ohlmann A, Reber SO. Short-term psychosocial stress protects photoreceptors from damage via corticosterone-mediated activation of the AKT pathway. *Exp Neurol.* 2014;252:28–36.
 43. Oliveira L, dos S, da Silva LP, da Silva AI, Magalhães CP, de Souza SL, de Castro RM. Effects of early weaning on the circadian rhythm and behavioral satiety sequence in rats. *Behav Proc.* 2011;86(1):119–124. Rowan S, Taylor A. The role of microbiota in retinal disease. In: Ash JD, Anderson RE, LaVail MM, Bowes Rickman C, Hollyfield JG, Grimm C, editors. *Retinal Degenerative Diseases*. Cham: Springer International Publishing; 2018. p. 429–35.
 45. Cervia D, Catalani E, Casini G. Neuroprotective peptides in retinal disease. *J Clin Med [Internet]*. 2019;8(8):1146.
 46. Léveillard T, Sahel J-A. Rod-derived cone viability factor for treating blinding diseases: from clinic to redox signaling. *Sci Transl Med.* 2010;2(26):26ps16–26ps16.
 47. Yu W, Mookherjee S, Chaitankar V, et al. Nrl knockdown by AAV-delivered CRISPR/Cas9 prevents retinal degeneration in mice. *Nat Commun.* 2017;8(1):1–15.
 48. Organisciak DT, Vaughan DK. Retinal light damage: mechanisms and protection. *Prog Retin Eye Res.* 2010 Mar;29(2):113–134.
 49. Radu RA, Mata NL, Nusinowitz S, Liu X, Sieving PA, Travis GH. Treatment with isotretinoin inhibits lipofuscin accumulation in a mouse model of recessive Stargardt's macular degeneration. *Proc Natl Acad Sci USA.* 2003 Apr 15;100(8):4742–4747.

50. Campana AO, Burini RC, Outa AY, De Camargo JL. Experimental protein deficiency in adult rats. *Rev Bras Pesqui Med Biol.* 1975;8(3-4):221–226.
51. Rhodopsin - an overview | ScienceDirect Topics [Internet]. [cited 2020 Sep 7], Available from: <https://www.sciencedirect.com/topics/neuroscience/rhodopsin>.
52. Auerbach E, Guggenheim K, Kaplansky J, Rowe H. Effect of protein depletion on the electric response of the retina in albino rats. *J Physiol.* 1964;172(3):417–424.
53. Degerud EM, Manger MS, Strand TA, Dierkes J. Bioavailability of iron, vitamin A, zinc, and folic acid when added to condiments and seasonings. *Ann N Y Acad Sci.* 2015 Nov;1357(1):29–42.
54. Gano LB, Patel M, Rho JM. Ketogenic diets, mitochondria, and neurological diseases. *J Lipid Res.* 2014 Nov;55(11):2211–2228.
55. Prince A, Zhang Y, Croniger C, Puchowicz M. Oxidative metabolism: glucose versus ketones. In: Van Huffel S, Naulaers G, Caicedo A, Bruley DF, Harrison DK, editors. *Oxygen Transport to Tissue XXXV*. New York, NY: Springer; 2013. p. 323–328.

Supplementary Material

Supplementary Movie S1. WT-W21-SC. Whole mount retina leaflet from a WT mouse that was on standard chow from PD21 to PD50. Red corresponds to cone arrestin staining, whereas blue corresponds to DAPI staining. Confocal images were processed by the Imaris 9.5.1 software.

Supplementary Movie S2. rd-W14/15-KLP. Whole mount retina leaflet from a rd10 mouse that was on the ketogenic & low protein diet from PD14/15 to PD50. Red corresponds to cone arrestin staining, whereas blue corresponds to DAPI staining. Confocal images were processed by the Imaris 9.5.1 software.

Supplementary Movie S3. rd-W14/15-SC. Whole mount retina leaflet from a rd10 mouse that was on standard chow from PD14/15 to PD50. Red corresponds to cone arrestin staining, whereas blue corresponds to DAPI staining. Confocal images were processed by the Imaris 9.5.1 software.